The Influence of Episodic Shallow Magma Degassing on Heat and Chemical Transport in Volcanic Hydrothermal Systems

Kewei Chen, Hongbin Zhan, Erick R. Burns, Steven E. Ingebritsen, Pierre Agrinier

AGU100 ADVANCING EARTH AND SPACE SCIENCE

Geophysical Research Letters

RESEARCH LETTER
10.1002/2017GL076449

Key Points:
- Analysis of episodic chemical and heat addition to groundwater provides insight into volcanic processes
- Joint analysis of chloride and temperature records from springs places constraints on the timing of magmatic degassing
- The frequency and duration of heat addition episodes and the distance and flow rate to springs control the thermal response at springs

Supporting Information:
- Supporting Information S1

Correspondence to:
H. Zhan,
zhan@geos.tamu.edu

Citation:
Chen, K., Zhan, H., Burns, E. R., Ingebritsen, S. E., & Agrinier, P. (2018). The influence of episodic shallow magma degassing on heat and chemical transport in volcanic hydrothermal systems. *Geophysical Research Letters*, *45*, 3068–3076. https://doi.org/10.1002/2017GL076449

Received 20 NOV 2017
Accepted 27 MAR 2018
Accepted article online 31 MAR 2018
Published online 13 APR 2018

The Influence of Episodic Shallow Magma Degassing on Heat and Chemical Transport in Volcanic Hydrothermal Systems

Kewei Chen[1], Hongbin Zhan[1], Erick R. Burns[2], Steven E. Ingebritsen[3], and Pierre Agrinier[4]

[1]Department of Geology and Geophysics, Texas A&M University, College Station, TX, USA, [2]U.S. Geological Survey, Portland, OR, USA, [3]U.S. Geological Survey, Menlo Park, CA, USA, [4]Institut de Physique du Globe de Paris, Paris, France

Abstract Springs at La Soufrière of Guadeloupe have been monitored for nearly four decades since the phreatic eruption and associated seismic activity in 1976. We conceptualize degassing vapor/gas mixtures as square-wave sources of chloride and heat and apply a new semianalytic solution to demonstrate that chloride and heat pulses with the same timing and duration result in good matches between measured and simulated spring temperatures and concentrations. While the concentration of chloride pulses is variable, the local boiling temperature of 96°C was assigned to all thermal pulses. Because chloride is a conservative tracer, chloride breakthrough is only affected by one-dimensional advection and dispersion. The thermal tracer is damped and lagged relative to chloride due to conductive heat exchange with the overlying and underlying strata. Joint analysis of temperature and chloride allows estimation of the onset and duration of degassing pulses, refining the chronology of recent magmatic intrusion.

Plain Language Summary Between eruptions, volcanoes continue to produce gases and water vapor associated with the cooling of magma (molten rock) deep beneath the volcano. These deep processes discharge gas and vapor (fumaroles) and heat the groundwater flowing through the volcano. Volcanic gases and vapors also contribute chemicals to the groundwater. Where groundwater leaves the volcano at springs, temperature and chemical measurements can be used to better understand the history of magmatic activity beneath the volcano. Understanding the history of volcanic processes aids volcanologists (scientists who study volcanoes) in understanding what conditions precede violent eruptions that might result in catastrophe.

1. Introduction

The phreatic eruptions that occurred in 1976–1977 at La Soufrière of Guadeloupe led to the establishment of a comprehensive volcano-monitoring network by the "Observatoire Volcanologique et Sismologique de La Soufrière de Guadeloupe". Thermal springs, fumaroles, and acid ponds have been monitored since 1979, along with permanent monitoring of seismic events and deformation. Fumarolic activity on the summit vanished almost completely by 1981, and the temperature and geochemical anomalies (deviations from background) observed at the springs diminished gradually from 1979 to 1992. Some fumaroles were reactivated after 1992, and HCl-rich H_2O vapor reappeared in late 1997. Those phenomena imply intrusion of new magma around 1992 (Boichu et al., 2011; Villemant et al., 2014). The evidence of magmatic influence, such as observed geochemical anomalies at springs, continues today.

Past studies have demonstrated that the geochemical anomalies in the springs (Cl or He isotopes and the F/Cl/Br/I/S chemistry) are of magmatic origin (Li et al., 2015; Ruzie et al., 2012; Villemant et al., 2005, 2014). The interpretation of spring temperature data has been more qualitative, in part due to lack of information about the subsurface structure, and in part because measureable temperature response occurs at only a few springs. However, understanding heat transport in the hydrothermal system is important since the thermal response reflects the input of magmatic fluid and mechanisms of eruption.

Recent geophysical surveys have greatly improved our understanding of the hydrothermal system, resulting in a physical model that describes the transport of both magmatic heat and chemicals (Rosas-Carbajal et al., 2016, 2017; Zlotnicki et al., 2006). Using this new model, we expand upon the previous chemical model of Villemant et al. (2005) to demonstrate that joint quantitative analysis of heat and conservative tracers allows refined estimation of the posteruptive degassing history of La Soufrière volcano. In addition, we analyze

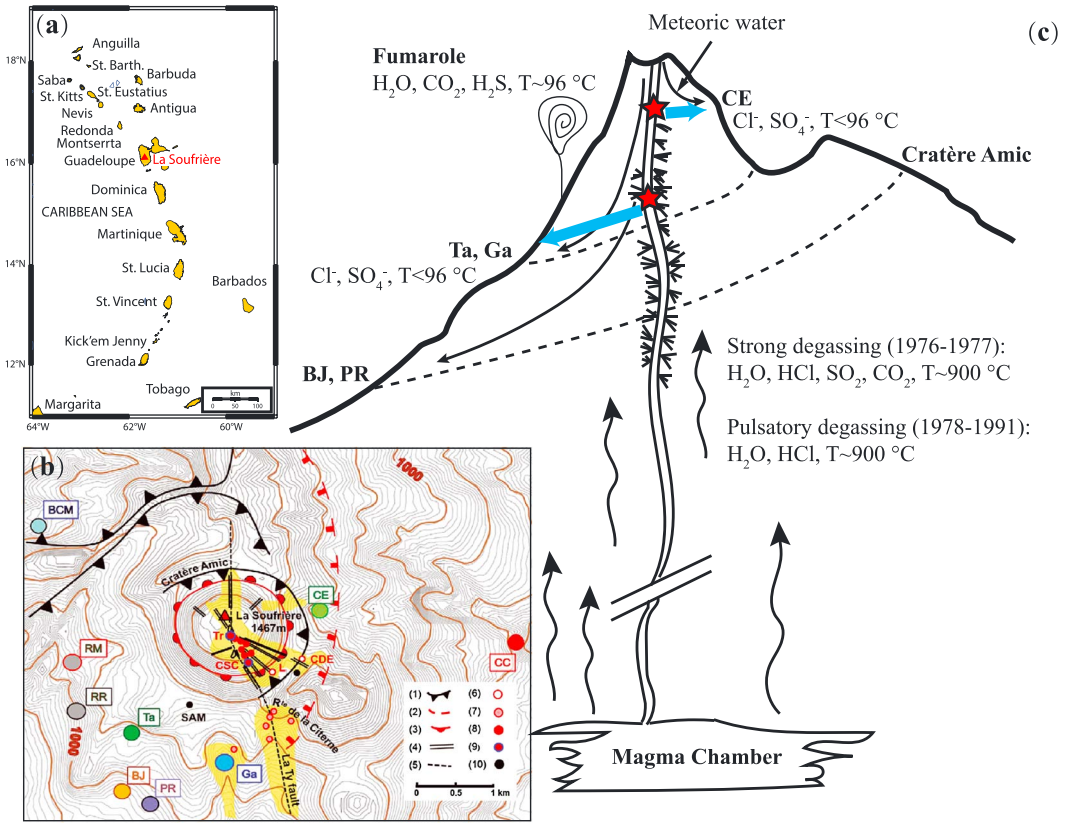

Figure 1. (a) Map showing the Caribbean volcanic arc with the location of La Soufrière volcano. (b) Contour map near the summit of La Soufrière volcano. Symbols in the contour map: (1) flank collapse scars, (2) La Grande Découverte Caldera, (3) La Soufrière dome, (4) summit fractures, (5) La Ty fault system, (6) 1976–1977 fumaroles active until 1981, (7) La Ty fumarolic field (weakly active until 1997), (8) summit fumaroles active since 1997, (9) fumaroles with intermittent acid lakes, and (10) Savane à Mulets (SAM) and Col de l'Echelle (CDE) wells. The hydrothermally altered zone is yellow, and thermal springs are indicated by large labeled circles (modified from Villemant et al., 2014). (c) Conceptual model for pulsatory degassing into near-surface aquifers at La Soufrière dome. Recharge occurs on the updip side of the hydrothermal alteration zones, with some possible recharge from the "meteoric water" lines. Red star, the zone of interaction between aquifer and volcanic gases; blue arrow, flow path; dashed line, outline of the deep hydrothermal system; solid line connecting magma reservoir and dome, eruptive conduit.

the combination of spring flow path properties and episodic heat flow that results in detectable thermal anomalies at springs.

2. Geological Setting

La Soufrière volcano is located on the island Basse Terre in Guadeloupe (Figure 1) and attains a maximum elevation of 1,470 m above mean sea level. Many thermal springs occur in or near the Cratère Amic structure, including Carbet Echelle (CE), Tarade (Ta), Bains Jaunes (BJ), Pas du Roy (PR), Galion (Ga), Ravine Marchand (RM), and Ravine Roche (RR), all of which are at high altitudes between ~950 and ~1,170 m above mean sea level and at a maximum distance of 1.2 km from the summit (Figure 1). Other more-distant springs, including Chute du Carbet (CC), Bains Chauds du Matouba (BCM), and Habitation Revel (HR), occur about 2–3 km from the dome.

Springs exhibit a gradation in response as a function of distance from the volcano. Only the spring that is nearest to the summit, CE, exhibits both strong geochemical and temperature anomalies. Springs at intermediate distance, such as Ga and BJ, capture much smoother Cl pulses (the result of dispersion), with a temperature response that is both lagged and significantly damped. The most distant springs, CC and BCM, show long-term thermal responses that may be confounded by regional hydrogeologic variation or climate variability, and only the CC spring exhibited the Cl response indicative of volcanic gas/vapor interaction. For the

work herein, CE, Ga, and CC are selected for investigation of the role of time and distance on the thermal and Cl pulses, thereby representing a range of distances from degassing heat source to spring outflow (~75, ~650, and ~2.5 km, respectively: Villemant et al., 2005).

The lava dome has been mapped geophysically, and individual aquifer flow horizons have been estimated for each spring, largely by mapping high electrical-conductivity pore-filling hydrothermal-alteration minerals that form layers that result in the perching and lateral flow of groundwater (Rosas-Carbajal et al., 2016, 2017; Zlotnicki et al., 2006). A mapped 150-m wide hydrothermally altered zone, with high electrical conductivity (larger than 1 S/m), lies about 150 m below the surface and is likely the main aquifer that transmits groundwater past the eruptive conduit to Ga spring (Rosas-Carbajal et al., 2016; Zlotnicki et al., 2006). The aquifers for springs CE and CC are likely more than 100 m below the surface. The average flow rate of Ga spring is 7.8 l/min between 1979 and 1995, and for spring CE, the average flow rate since 1995 is 7.1 l/min (Villemant et al., 2005). No flow rate data is available for spring CC. The average annual land surface temperature at the base of the lava dome is nearly constant at about 20°C, and the thermal gradient in the conductive domain beneath the hydrothermal systems is ~170°C/km (Zlotnicki et al., 1992).

Fluid discharged from the spring is a combination of meteoric water and magmatic gases. Within the eruptive conduit (Figure 1c), high-temperature gas and vapor emission occurs in pulses and is related to a two-step magma degassing process characterized by the initial rapid release of HCl-rich H_2O vapor during emplacement of new magma, followed by protracted release of gases and vapor at diminishing rates during crystallization of the newly emplaced magma (Boichu et al., 2008). This pulsatory magma degassing has previously been conceptualized as a series of instantaneous pulses that release hot gas and vapors (including HCl) to the overlying aquifer(s), causing observed thermal and geochemical anomalies, including a conservative Cl pulse (Villemant et al., 2005).

3. Conceptual Model and Method of Analysis

We assume that each aquifer discharging to a spring receives pulses of Cl and heat from the eruptive conduit at a discrete location under the volcano, after which Cl is transported conservatively. Heat is added conductively to the aquifer from below along the groundwater flow path, and the aquifer is insulated from the land surface above by the vadose zone. While the instantaneous chemical addition models of Villemant et al. (2005) ensure that the total Cl mass added is correct, instantaneous models require unrealistic infinite spikes in concentration/temperature near the zone of chemical/heat addition. Instead, we conceptualize the input pulses as square waves with physically realistic magnitude where timing is the same for all springs and for both Cl and heat. Use of a square wave has two advantages. First, degassing is not instantaneous, resulting in a period of interaction with the aquifer that is now explicitly represented. Second, the amplitude of the heat pulse is constrained by the local boiling point (measured near the summit at the 96°C boiling acid pond and fumaroles which range between 94 and 120°C), where the process of boiling prevents groundwater temperature from being arbitrarily high, providing a constraint on pulse duration. The number of pulses, the starting times and duration, and the magnitude of the pulses were adjusted to calibrate the model to measurements. Magnitude of each Cl pulse was adjusted so that mass delivered as HCl balanced with measured Cl. A constant temperature of 96°C was assumed for all pulses. This uniformly high temperature assumes that boiling and condensation of vapor are widespread within the part of the aquifer that is interacting with volcanic gases and vapors. Temperatures do not exceed boiling temperatures, because excess heat is consumed by the latent heat of vaporization.

Assuming single-phase lateral transport of chloride and heat in the aquifer simplifies calculations and is also consistent with the physics of the system as we understand it. Significant lateral chloride transport by a vapor phase is unlikely, because the volatility of chloride in low-pressure vapor is negligibly small. Lateral heat transport by a vapor phase will also be negligibly small, because of the large density contrast between liquid and vapor phases. The density contrast between liquid water and water vapor (a factor of about 10^3 at pressures of a few bars) dictates a strong tendency for subvertical upward vapor flow into the overlying unsaturated zone, so that vapor will tend to leave the system above where it is first generated. As some water vapor condenses along its upward flow path, condensate will tend to flow subvertically downward through the unsaturated zone, providing a narrow zone of contribution to the aquifer. Lateral flow of heavier-than-air noncondensible gases (dominated by CO_2) is physically possible in the unsaturated zone above the water

table. However, the fumarole temperature—near the local boiling point for pure water—indicates minor CO_2 content; the vapor is likely >98% H_2O by mass. Despite the high water content of the vapor, measured spring flow rate and chemistry indicate that condensed vapor is a very small fraction of the total groundwater flowing beneath La Soufrière volcano (Villemant et al., 2014).

For heat transport, we consider both heat advection and dispersion within the aquifer along the flow path and conductive heat exchange between the aquifer and the vadose zone and basal layers (Burns et al., 2017). The governing equation for heat transport in the aquifer with multiple heat pulses is

$$\Gamma_{aq}\frac{\partial T_{aq}}{\partial t}+u\rho_w c_w\frac{\partial T_{aq}}{\partial x}-\sigma_a\frac{\partial^2 T_{aq}}{\partial x^2}+\frac{\sigma_{vz}}{h_{aq}}\frac{\partial T_{vz}}{\partial z}\bigg|_{z=h_{vz}}-\frac{\sigma_{bu}}{h_{aq}}\frac{\partial T_{bu}}{\partial z}\bigg|_{z=h_{vz}+h_{aq}}=0, \tag{1a}$$

$$T_{aq}(x=0,t)=T_{r,j}(t), t\in\left[t_{j-1},t_j\right), j=1,2,\ldots,P, \tag{1b}$$

where T is the temperature with "*aq*," "*vz*," and "*bu*" corresponding to aquifer, vadose zone, and basal unit, respectively; Γ is the volumetric heat capacity; u is the groundwater flow velocity; ρ_w and c_w are the water density and specific heat, respectively; σ is the bulk thermal conductivity; h is the layer thickness; and $T_{r,j}$ is the temperature of pulses at the point of interaction between the groundwater and the volcanic gases. Temperature alternates between hot pulse temperature and cool background temperature, and P is the number of periods used to define heat pulses. The heat exchange between the vadose zone and the aquifer occurs at $z = h_{vz}$ where $z = 0$ is at the land surface, and the heat exchange between the basal unit and the aquifer is at $z = h_{vz} + h_{aq}$. The heat flow model is pseudo-2D, in that the one-dimensional subhorizontal groundwater-flow along the aquifer is assumed to be well mixed, and subvertical conductive heat exchange with the overlying and underlying geology is assumed to be orthogonal to groundwater-flow. Burns et al. (2016, 2017) provides an expanded discussion and limitations associated with this approach. Simulation results will be minimally sensitive to variations in vadose thickness, because vadose thickness is large compared with the heat penetration depth that occurs over the simulation period of a decade (~30 m), as estimated by the 1-D conduction solution,

$$T_{vz}=\Delta T\,\mathrm{erfc}\left(\frac{d}{2}\sqrt{\frac{\Gamma_{vz}}{\sigma_{vz}t}}\right), \tag{2}$$

where ΔT is the step change of aquifer temperature and d is vertical distance away from the aquifer (Carslaw & Jaeger, 1986).

For Cl transport in the aquifer, we assume that Cl is conservative (i.e., no diffusion into the overlying/underlying geology and no chemical reactions), giving the one-dimensional equation for advection and dispersion along the flow path,

$$\frac{\partial C}{\partial t}+u\frac{\partial C}{\partial x}-D\frac{\partial C^2}{\partial x^2}=0, \tag{3a}$$

$$C(x=0,t)=C_{r,j}(t), t\in\left[t_{j-1},t_j\right), j=1,2,\ldots,P., \tag{3b}$$

where D is the dispersion coefficient and $C_{r,j}$ is the constant concentration used to define pulses (alternating between pulse magnitude and background concentration). The transient solutions for heat transport and Cl transport are developed in the supporting information, with the solutions given as equations (S20) and (S24).

For implementation of the solutions, other model assumptions include the following: (1) all three springs experience degassing pulses at the same time (in response to the same seismo-volcanic events), but chloride loading rate varies as a function of heterogeneous emplacement of magma and geology between magma and aquifers (i.e., total amount of Cl delivered to each flow path can vary); (2) the groundwater and hot fluid (gas/vapor/condensate mixture) are instantaneously well mixed in the aquifer; (3) the groundwater flow rates are constant for the period of simulation 1979–1992 (Villemant et al., 2005); (4) the high-temperature gas/vapor mixtures increase the fluid temperature to the boiling point instantaneously; and (5) the influence of variable fluid density, viscosity, and specific heat is not significant. All model parameters were extracted from published values (Eppelbaum et al., 2014; Rosas-Carbajal et al., 2016; Villemant et al., 2005; Villemant et al., 2014) and are summarized in Table S1 of the supporting information.

To calibrate the model, we adopt this workflow: (1) use a steady temperature distribution along each aquifer estimated by the steady solution of Burns et al. (2016) as the initial condition before pulsatory injection,

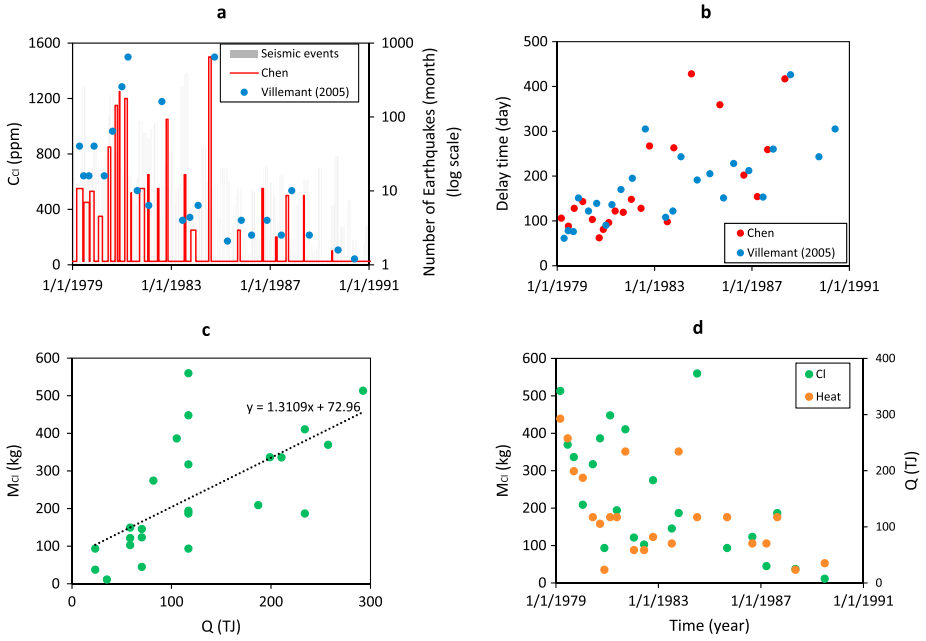

Figure 2. Comparison between the square-wave chloride source (Chen, this study) and instantaneous-source used by Villemant et al. (2005), and estimated Cl mass and amount of heat in individual pulses. (a) Plot showing that Cl pulse concentration estimated by the current study and Villemant et al. (2005) is generally correlated with seismicity and each other. Red line: the square-wave chloride pulses. Blue dot: instantaneous sources (scaled for comparison to a similar range as the square wave) inferred by Villemant et al. (2005). Gray line: number of detected earthquakes for comparison with degassing loading. (b) The time between the starting points of successive square-wave pulses showing that pulse frequency decreases over time. (c) Crossplot of the Cl mass M_{Cl} (kg) and amount of heat Q (TJ) delivered in individual pulses, showing that heat and Cl delivered in each pulse is correlated, where M_{Cl} = flow rate × pulse duration × pulse concentration and Q = volumetric heat capacity of water × flow rate × pulse duration × (local boiling temperature-background recharge temperature). (d) Plot of M_{Cl} and Q delivered in individual pulses over time, showing the decrease in heat and Cl delivered by individual pulses over time.

allowing us to simulate background conductive geothermal heat flow into the aquifer along the groundwater flow path; (2) estimate the number and timing of Cl pulses by matching the peak arrival times at each spring (because peak is a good indicator of advective flow); (3) estimate the duration for each pulse to balance total heat delivered to CE spring assuming a constant 96°C source temperature; and (4) estimate Cl concentrations of individual pulses necessary to balance measured Cl concentration at springs.

Initial conditions were developed by estimating long-term temperature and Cl conditions at the springs. The lowest Cl values are assumed to be approximately the background steady value. Similarly, because degassing adds heat, the lowest temperatures were used to estimate long-term background temperature. Background conductive heat flow from beneath the aquifer is estimated to be 0.34 W/m^2 by using the measured thermal gradient of Zlotnicki et al. (~170°C/km, 1992), and a representative value of thermal conductivity for andesite (1.97 W/mK; Eppelbaum et al., 2014).

4. Results

The long-term steady background spring temperatures (i.e., no influence of degassing pulses) are estimated to be 21, 38, and 43°C for CE, Ga, and CC springs, respectively, under the assumptions that the 1976 phreatic eruption did not yet have a strong thermal effect on the two longer flow-path springs (Ga and CC) by 1979 and that by 1991, the CE spring temperature was asymptotically trending toward background temperature. Using the estimated basal heat flow (0.34 W/m^2) and the long-term steady background spring temperatures, background groundwater inflow temperatures at the eruptive conduit (i.e., no influence of degassing pulses) were computed to be 20.5, 35.6, and 37.5°C, for CE, Ga, and CC springs flow paths, respectively.

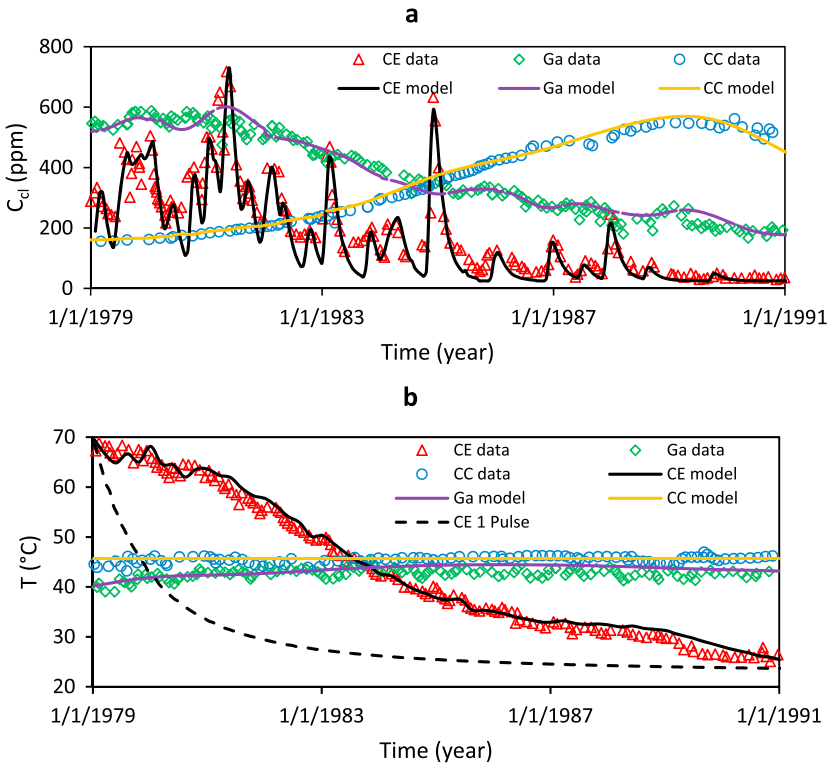

Figure 3. Measured and simulated Cl concentrations and temperatures at springs of CE (proximal to the summit, ~75 m distant), Ga (intermediate to the summit, ~650 m), and CC (distal to the summit, ~2,800 m). (a) CE spring Cl concentration responds quickly to the degassing activity (approximately three-month delay), and the delay times for Ga and CC spring are ~2.1 years and ~9 years, respectively. (b) Measured and simulated temperature: CE spring temperature decays with the decreasing pulse frequency; Ga spring temperature increases ~3°C from 1979 to 1982 and then remains constant; CC spring temperature is constant at 45°C from 1979 to 1991. Dashed line: simulated CE spring temperature assuming no episodic degassing pulse heating except the heating from the first one-year pulse. The difference between the CE solid and dashed lines is the result of heat pulses to the aquifer from degassing.

To represent the period of decreasing volcanic activity after 1976, we used 26 square waves to match the measured 1979–1992 thermal and chemical response at the springs (Figure 2a and Table S2). For our analysis, a single relatively long-duration one-year pulse was used to represent the phreatic eruption, perturbing the long-term steady chloride and temperature values and giving a good match to the conditions when measurements started in 1979. It is possible that multiple degassing events occurred before 1979 and that the effect of such degassing events in terms of thermal response at the springs would be equivalent to an individual pulse that lasts for about one year.

Our results are similar to those of Villemant et al. (2005), who for the same 1979–1992 period used 27 instantaneous Cl pulses to estimate the timing of degassing events and total chloride introduced to the aquifers. Both sets of results display a reduction in frequency of degassing events over time (Figure 2b) and less addition of chloride to the aquifers over time. The mass of Cl introduced in an individual pulse is proportional to the amount of heat in the same pulse (Figure 2c), and there is a decreasing trend in mass and heat delivered by individual pulses over time (Figure 2d).

Figure 3a shows measured and the new simulated chloride concentrations for CE, Ga, and CC springs, and Figure 3b shows corresponding measured and simulated temperature. Compared to the previous method of using instantaneous Cl spikes to understand transport to springs (Villemant et al., 2005), jointly simulating the breakthrough of temperature and Cl estimates the duration of degassing pulses and also provides physically realistic values of temperature and Cl at all points within the aquifers. By definition, instantaneous spikes require arbitrarily high concentrations and temperatures to deliver the correct amount of total mass and heat, respectively. However, because the upper limit of aquifer temperature is constrained by

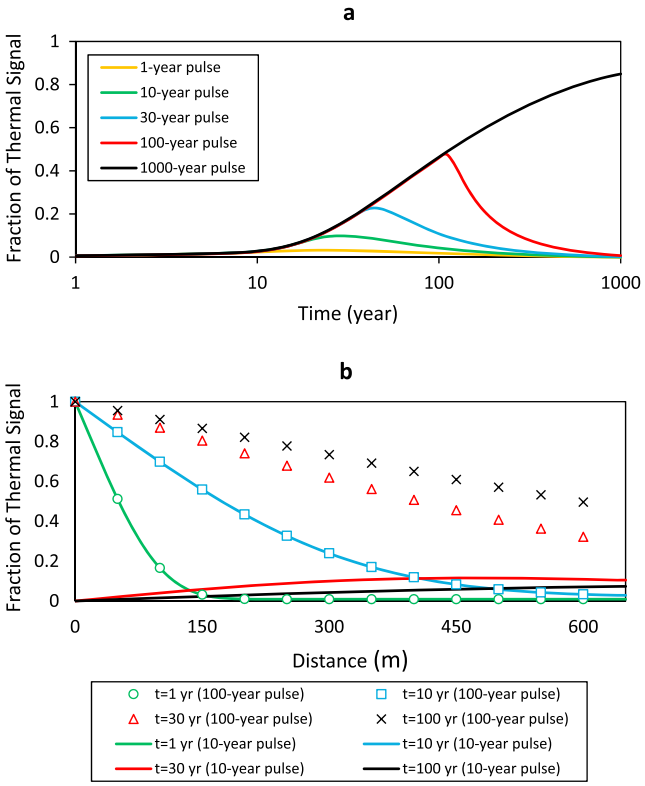

Figure 4. BTCs and temperature profiles generated for different heat pulse durations using the model for Ga spring (x = 650 m). Fraction of thermal signal = (observed temperature at x − steady temperature at x)/(local boiling temperature − steady temperature at x). (a) BTCs at Ga spring with 1-, 10-, 30-, 100-, and 1,000-year pulse duration. After 1000 years the full thermal signal has not reached the Ga spring despite having an estimated advective traveltime of ~2.1 years. (b) The distribution of temperature along the groundwater flow path at four different times, 1-, 10-, 30-, and 100-year, resulting from two different pulse durations. The 10-year pulse is shown with solid lines, and the 100-year pulse is shown with discrete symbols. For times less than 10 years, the profiles are identical. Between 10 and 100 years, temperatures continue to rise for the 100-year pulse, but the 10-year pulse quickly damps and translates toward the spring (distance = 650 m).

boiling/condensation, minimum pulse duration is well defined by the total heating necessary to replicate measured spring temperatures, given this upper limit temperature. Because Cl is conservative, the center of the square wave is well constrained (within ~0.01 years). Using the pulse duration estimated from the temperature signal, the measured total mass of Cl is used to estimate the magnitude of the Cl pulse.

CE spring is very sensitive to pulsatory degassing (Figure 3a), and individual past degassing events are recorded in the peaks of the Cl time series (i.e., the memory effect of Villemant et al., 2005). The temperature record has even longer memory (Figure 3b), with temperature constraining estimates of pulse duration, and with conductive heat exchange resulting in lagged and damped long-term response to degassing episodes. The Cl concentration data from CE spring cannot help us infer degassing activity before 1979 due to the short system memory resulting from rapid advection of a conservative tracer (approximately three-month advective traveltime, obtained from the ratio of the aquifer length to groundwater velocity). For Ga spring, with a memory of ~2.1 years, the first peak of the Cl time series reflects degassing activity as early as 1976–1977. Note that due to the longer transit time, while individual peaks are still discernable, the overall Cl response is starting to resemble a single large broad bulge, where dispersion is merging individual pulses. The broad decline in Cl concentration over the period 1979–1992 reflects both the reduction in pulse frequency and in individual pulse Cl concentration (Figure 2d). At CC spring, with an advective time of ~9 years, the Cl peak is correspondingly later in time, and the curve is even smoother than for Ga due to the additional dispersion over distance and time.

Temperature at springs is lagged and damped due to conductive heat exchange with the overlying and underlying geology. Damping of the thermal signal is partly the result of the time-lag physics, but also heat loss to ambient conditions, so that total heat arriving at the spring is less than the pulsatory heat addition to groundwater (i.e., heat is not conservative). The simulated temperature for the proximal CE spring matches the measurements well, supporting the conceptual models of heat delivery and transport and demonstrating that temperatures exceeding the boiling point are not required to explain the temperature signal at springs. The reasonable match to temperature for all three springs demonstrates the importance of flow path length on controlling thermal signals.

To underscore the importance of total heat added by pulses, temperature was simulated at CE spring assuming that there were no heat pulses following the 1976–1977 phreatic eruption (dashed line on Figure 3b). The difference between the solid and dashed lines for CE spring shows the influence of pulsatory heating, and the area between the curves is the difference in heat delivered to the spring as a result of degassing pulses.

Whether a pulse is a single long pulse, or a series of pulses closely spaced in time, the resulting heat signal at springs will be lagged and damped, possibly to the point of being undetectable. For La Soufrière springs, because pulse temperatures are constrained to be ~96°C, the recorded temperature at each spring is only a function of duration of the pulse. Figure 4a displays breakthrough curves (BTCs) for a range of pulse durations using the hydrogeologic setting of Ga spring. The one-year pulse peak is weakened by more than 95% at the Ga spring. The longer the pulse duration, the larger the amplitude and the longer it takes for the disturbed temperature to return to steady state. Figure 4b shows temperature profiles along the groundwater flow path contributing to Ga spring at different times for both 10-year and 100-year pulses. For the 100-year pulse, the temperature at Ga spring continuously increases throughout the 100-year period. Conversely, for the 10-year pulse, the spring temperature first increases and then decreases. The 30-year

profile for the 10-year pulse shows the effects of damping and translation along the groundwater flow-path after the pulse is discontinued. The 100-year profile for the 10-year pulse shows additional damping and translation and shows that heat stored from a 10-year pulse will have lasting but relatively small effects on spring temperature.

5. Discussion and Conclusions

Our model demonstrates that a single sequence of magma degassing events following the 1976–1977 phreatic eruption can explain the observed geochemical and temperature signals for a range of La Soufrière springs. The chloride time series records episodic degassing events, with lag times consistent with measured spring flow rates. Relative to chloride, heat is significantly lagged and damped, and for short-duration degassing events, thermal responses will not be detectable at distal springs.

While the physical model of the cycle of magma cooling, crystallization, and degassing has been previously developed and is correlated to the time series of Cl observed at springs, the transport process of the volatiles between the starting point, magma, and the ending point, spring, is less well known (Boichu et al., 2008; Boichu et al., 2011; Villemant et al., 2005). Our model partially fills the gap by demonstrating that limited-duration pulses with physically realistic rates of exchange between vapor and aquifers can explain measured spring responses. Because aquifer temperature must be at or below boiling, including spring temperature in our analysis provided a constraint on degassing pulse minimum duration.

The basal conductive heat flux beneath the volcano is estimated to be about 0.34 W/m^2 based on the measured geothermal gradient, which is in the range of reasonable values (e.g., Blackwell et al., 1990; Burns et al., 2017; Hochstein, 1995; Ingebritsen et al., 1989; Morgan et al., 1977; Williams & DeAngelo, 2008, 2011). The regional heat flux on the crest of the Lesser Antilles arc, 0.1 W/m^2 (Manga et al., 2012), is much lower than that nearer the volcano, where it is elevated by conduction from the underlying magma reservoir. During degassing events heat delivered to groundwater advectively by vapors is much larger than conductively delivered heat flow, and the total amount of heat delivered from individual degassing events can be estimated from the duration and magnitude of the thermal input pulses.

We developed a semianalytic solution to transport of Cl and heat in La Soufrière volcano's hydrothermal system that assumes geothermal heating of groundwater from recharge areas to springs, allowing us to evaluate the influence of episodic heating in a narrow region of interaction. During periods of magma degassing, heat is added to groundwater via interaction with volcanic gases and vapor as groundwater flows beneath the volcanic dome. Considering Cl and heat together allows us to define a single set of degassing events (i.e., pulse durations) that explains spring response for both Cl and temperature as a function of distance from the dome. Further, the resulting set of degassing pulses does not require physically unreasonable values of temperature or Cl at any location within the hydrothermal system.

Acknowledgments
The authors thank Chi-Yuen Wang and Benoit Villemant for their helpful review comments. Seismic data, temperature, and chemical spring monthly data were collected by OVSG-IPGP team since 1978. The monthly temperature and Cl data of CE, Ga, and CC springs between 1979 and 1992 are provided in the supporting information (Table S3). Funding for Erick R. Burns was provided by the U.S. Department of Energy Geothermal Technologies Program (EERE award number DE-EE0007169), the USGS Energy Resources Program, and the USGS Water Availability and Use Science Program.

References

Blackwell, D. D., Steele, J. L., Kelley, S., & Korosec, M. A. (1990). Heat flow in the state of Washington and thermal conditions in the Cascade range. *Journal of Geophysical Research*, *95*(B12), 19,495–19,516.

Boichu, M., Villemant, B., & Boudon, G. (2008). A model for episodic degassing of an andesitic magma intrusion. *Journal of Geophysical Research*, *113*, B07202. https://doi.org/10.1029/2007JB005130

Boichu, M., Villemant, B., & Boudon, G. (2011). Degassing at La Soufriere de Guadeloupe volcano (Lesser Antilles) since the last eruptive crisis in 1975–77: Result of a shallow magma intrusion? *Journal of Volcanology and Geothermal Research*, *203*(3–4), 102–112. https://doi.org/10.1016/j.jvolgeores.2011.04.007

Burns, E. R., Ingebritsen, S. E., Manga, M., & Williams, C. F. (2016). Evaluating geothermal and hydrogeologic controls on regional groundwater temperature distribution. *Water Resources Research*, *52*(2), 1328–1344. https://doi.org/10.1002/2015WR018204

Burns, E. R., Zhu, Y. H., Zhan, H. B., Manga, M., Williams, C. F., Ingebritsen, S. E., & Dunham, J. B. (2017). Thermal effect of climate change on groundwater-fed ecosystems. *Water Resources Research*, *53*, 3341–3351. https://doi.org/10.1002/2016WR020007

Carslaw, H. S., & Jaeger, J. C. (1986). *Conduction of heat in solids*. Oxford, UK: Clarendon Press.

Eppelbaum, L., Kutasov, L., & Pilchin, A. (2014). *Applied geothermics*. Berlin, Heidelberg: Springer. https://doi.org/10.1007/978-3-642-34023-9

Hochstein, M. P. (1995). Crustal heat transfer in the Taupo Volcanic Zone (New Zealand): Comparison with other volcanic arcs and explanatory heat source models. *Journal of Volcanology and Geothermal Research*, *68*(1-3), 117–151. https://doi.org/10.1016/0377-0273(95)00010-R

Ingebritsen, S. E., Sherrod, D. R., & Mariner, R. H. (1989). Heat flow and hydrothermal circulation in the Cascade range, north-central Oregon. *Science*, *243*(4897), 1458–1462. https://doi.org/10.1126/science.243.4897.1458

Li, L., Bonifacie, M., Aubaud, C., Crispi, O., Desset, C., & Agrinier, P. (2015). Chlorine isotopes of thermal springs in arc volcanoes for tracing shallow magmatic activity. *Earth and Planetary Science Letters*, *413*, 101–110. https://doi.org/10.1016/j.epsl.2014.12.044

Manga, M., Hornbach, M. J., Friant, A. L., Ishizuka, O., Stroncik, N., Adachi, T., et al. (2012). Heat flow in the Lesser Antilles island arc and adjacent back arc Grenada basin. *Geochemistry, Geophysics, Geosystems*, *13*, Q08007. https://doi.org/10.1029/2012GC004260

Morgan, P., Blackwell, D. D., Spafford, R. E., & Smith, R. B. (1977). Heat flow measurements in Yellowstone Lake and the thermal structure of the Yellowstone Caldera. *Journal of Geophysical Research*, *82*(26), 3719–3732. https://doi.org/10.1029/JB082i026p03719

Rosas-Carbajal, M., Jourde, K., Marteau, J., Deroussi, S., Komorowski, J. C., & Gibert, D. (2017). Three-dimensional density structure of La Soufriere de Guadeloupe lava dome from simultaneous muon radiographies and gravity data. *Geophysical Research Letters*, *44*, 6743–6751. https://doi.org/10.1002/2017GL074285

Rosas-Carbajal, M., Komorowski, J. C., Nicollin, F., & Gibert, D. (2016). Volcano electrical tomography unveils edifice collapse hazard linked to hydrothermal system structure and dynamics. *Scientific Reports*, *6*(6), 29899. https://doi.org/10.1038/srep29899

Ruzie, L., Moreira, M., & Crispi, O. (2012). Noble gas isotopes in hydrothermal volcanic fluids of La Soufriere volcano, Guadeloupe, Lesser Antilles arc. *Chemical Geology*, *304*, 158–165.

Villemant, B., Hammouya, G., Michel, A., Semet, M. P., Komorowski, J. C., Boudon, G., & Cheminee, J. L. (2005). The memory of volcanic waters: Shallow magma degassing revealed by halogen monitoring in thermal springs of La Soufriere volcano (Guadeloupe, Lesser Antilles). *Earth and Planetary Science Letters*, *237*(3–4), 710–728. https://doi.org/10.1016/j.epsl.2005.05.013

Villemant, B., Komorowski, J. C., Dessert, C., Michel, A., Crispi, O., Hammouya, G., et al. (2014). Evidence for a new shallow magma intrusion at La Soufriere of Guadeloupe (Lesser Antilles) Insights from long-term geochemical monitoring of halogen-rich hydrothermal fluids. *Journal of Volcanology and Geothermal Research*, *285*, 247–277.

Williams, C. F., & DeAngelo, J. (2008). Mapping geothermal potential in the western United States. *Geothermal Resources Council Transactions*, *32*, 181–188.

Williams, C. F., & DeAngelo, J. (2011). Evaluation of approaches and associated uncertainties in the estimation of temperatures in the upper crust of the western United States. *Geothermal Resources Council Transactions*, *35*, 1599–1605.

Zlotnicki, J., Boudon, G., & Lemouel, J. L. (1992). The volcanic activity of La Soufriere of Guadeloupe (Lesser Antilles)—Structural and tectonic implications. *Journal of Volcanology and Geothermal Research*, *49*(1–2), 91–104. https://doi.org/10.1016/0377-0273(92)90006-Y

Zlotnicki, J., Vargemezis, G., Mille, A., Bruere, F., & Hammouya, G. (2006). State of the hydrothermal activity of Soufriere of Guadeloupe volcano inferred by VLF surveys. *Journal of Applied Geophysics*, *58*(4), 265–279. https://doi.org/10.1016/j.jappgeo.2005.05.004